J|A|C|S
ARTICLES

NMR-Based Structural Modeling of Graphite Oxide Using Multidimensional ^{13}C Solid-State NMR and ab Initio Chemical Shift Calculations

Leah B. Casabianca,[†] Medhat A. Shaibat,[†] Weiwei W. Cai,[‡] Sungjin Park,[‡] Richard Piner,[‡] Rodney S. Ruoff,[‡] and Yoshitaka Ishii*,[†]

Department of Chemistry, University of Illinois at Chicago, 845 West Taylor Street, Chicago, Illinois 60607, and Department of Mechanical Engineering and the Texas Materials Institute, The University of Texas at Austin, Austin, Texas 78712

Received April 15, 2009; E-mail: yishii@uic.edu

Abstract: Chemically modified graphenes and other graphite-based materials have attracted growing interest for their unique potential as lightweight electronic and structural nanomaterials. It is an important challenge to construct structural models of noncrystalline graphite-based materials on the basis of NMR or other spectroscopic data. To address this challenge, a solid-state NMR (SSNMR)-based structural modeling approach is presented on graphite oxide (GO), which is a prominent precursor and interesting benchmark system of modified graphene. An experimental 2D ^{13}C double-quantum/single-quantum correlation SSNMR spectrum of ^{13}C-labeled GO was compared with spectra simulated for different structural models using ab initio geometry optimization and chemical shift calculations. The results show that the spectral features of the GO sample are best reproduced by a geometry-optimized structural model that is based on the Lerf−Klinowski model (Lerf, A. et al. *Phys. Chem. B* **1998**, *102*, 4477); this model is composed of interconnected sp^2, 1,2-epoxide, and COH carbons. This study also convincingly excludes the possibility of other previously proposed models, including the highly oxidized structures involving 1,3-epoxide carbons (Szabo, I. et al. *Chem. Mater.* **2006**, *18*, 2740). ^{13}C chemical shift anisotropy (CSA) patterns measured by a 2D ^{13}C CSA/isotropic shift correlation SSNMR were well reproduced by the chemical shift tensor obtained by the ab initio calculation for the former model. The approach presented here is likely to be applicable to other chemically modified graphenes and graphite-based systems.

Introduction

Graphene, a single-atom thick layer of graphite, was first prepared over 30 years ago by thermal chemical vapor deposition on single-crystal metal substrates.[1] Due to the recent revisiting of this system as a new class of carbon nanomaterials having fascinating electronic transport[2] and structural properties,[3,4] graphene and other graphene-based materials have gained enormous attention. Chemical modifications of graphene have offered exciting paths to altering its novel functionality.[3−7] As new classes of modified graphenes are discovered, there will be a need for methods to determine their detailed chemical structures. Unfortunately, modified graphenes and graphite-based materials are often heterogeneous, noncrystalline, and insoluble. Conventional methods such as solution NMR and X-ray crystallography are thus limited as sources of structural information for such nanomaterials. Solid-state NMR (SSNMR) is a unique tool that can provide site-specific structural information for heterogeneous noncrystalline solids,[8−13] in some cases, in combination with ab initio calculations.[14−20] However, distinguishing different structural models of graphite- or graphene-based materials from NMR or other spectroscopic data has not been trivial.

Graphite oxide (GO) has attracted broad attention as a prominent precursor for mass production of single-layer graphene and chemically modified graphene and as an interesting model

[†] University of Illinois at Chicago.
[‡] The University of Texas at Austin.

(1) Patil, H. R.; Blakely, J. M. *J. Chem. Phys.* **1974**, *45*, 3806–3808.
(2) Novoselov, K. S.; Geim, A. K.; Morozov, S. V.; Jiang, D.; Zhang, Y.; Dubonos, S. V.; Grigorieva, I. V.; Firsov, A. A. *Science* **2004**, *306*, 666–669.
(3) Stankovich, S.; Dikin, D. A.; Dommett, G. H. B.; Kohlhaas, K. M.; Zimney, E. J.; Stach, E. A.; Piner, R. D.; Nguyen, S. T.; Ruoff, R. S. *Nature* **2006**, *442*, 282–286.
(4) Dikin, D. A.; Stankovich, S.; Zimney, E. J.; Piner, R. D.; Dommett, G. H. B.; Evmenenko, G.; Nguyen, S. T.; Ruoff, R. S. *Nature* **2007**, *448*, 457–460.
(5) Ruoff, R. *Nat. Nanotech.* **2008**, *3*, 10–11.
(6) Park, S.; Ruoff, R. S. *Nat. Nanotech.* **2009**, *4*, 217–224.
(7) Veca, L. M.; Lu, F. S.; Meziani, M. J.; Cao, L.; Zhang, P. Y.; Qi, G.; Qu, L. W.; Shrestha, M.; Sun, Y. P. *Chem. Commun.* **2009**, 2565–2567.
(8) Schmidt-Rohr, K.; Spiess, H. W. *Multidimensional Solid-state NMR and Polymers*; Academic Press, Inc.: San Diego, 1994.
(9) Hayes, S.; vanWullen, L.; Eckert, H.; Even, W. R.; Crocker, R. W.; Zhang, Z. M. *Chem. Mater.* **1997**, *9*, 901–911.
(10) Cai, W. W.; Piner, R. D.; Stadermann, F. J.; Park, S.; Shaibat, M. A.; Ishii, Y.; Yang, D. X.; Velamakanni, A.; An, S. J.; Stoller, M.; An, J. H.; Chen, D. M.; Ruoff, R. S. *Science* **2008**, *321*, 1815–1817.
(11) Ramamoorthy, A. *NMR Spectroscopy of Biological Solids*; CRC Press: Boca Raton, FL, 2005.
(12) Igumenova, T. I.; McDermott, A. E.; Zilm, K. W.; Martin, R. W.; Paulson, E. K.; Wand, A. J. *J. Am. Chem. Soc.* **2004**, *126*, 6720–6727.
(13) Chimon, S.; Shaibat, M. A.; Jones, C. R.; Calero, D. C.; Aizezi, B.; Ishii, Y. *Nat. Struct. Mol. Biol.* **2007**, *14*, 1157–1164.
(14) de Dios, A. C.; Oldfield, E. *Science* **1993**, *260*, 1491.

10.1021/ja9030243

of single-layer "graphene oxide";[21−27] we present a SSNMR-based structural modeling approach for analyzing its structure as a framework that is potentially applicable to a broad range of graphene-based systems. One of the crucial bottlenecks for the application of graphene-based systems in materials science is their mass production. Unlike graphite, GO can be dispersed into single-layer *graphene* oxide by sonication or simple stirring in water.[3] Since the resulting product can be further chemically modified into graphene or graphene-based systems,[27] a variety of studies on GO have been undertaken.[21−26,28] GO has also been used as a precursor to make graphene-based nanosheets,[27] graphene-based "paper" materials,[4,29−31] and polymer composite materials having embedded and modified graphene sheets.[3] Despite its significance, the structure of GO is still debated[21,23,25,28,32−34] more than 150 years after its first synthesis.[35] In particular, intense modeling efforts were very recently made for oxidized graphite layers,[21,23,25,28] yet a conclusive structure model has not been established. Uniformly ^{13}C-labeled GO was recently synthesized, allowing its ^{13}C−^{13}C connectivities to be determined for the first time by SSNMR.[10] Based on such results, a systematic approach to evaluate structural models is here undertaken involving direct comparison of experimental 2D ^{13}C SSNMR spectra with simulated 2D spectra obtained from ab initio calculations. The presented approach offers a novel means of evaluating various structural models by NMR without a priori knowledge of NMR signal assignments for modified graphene having a complex chemical network. This approach is also likely to open an avenue for NMR-based structural studies for a broad range of modified graphenes.

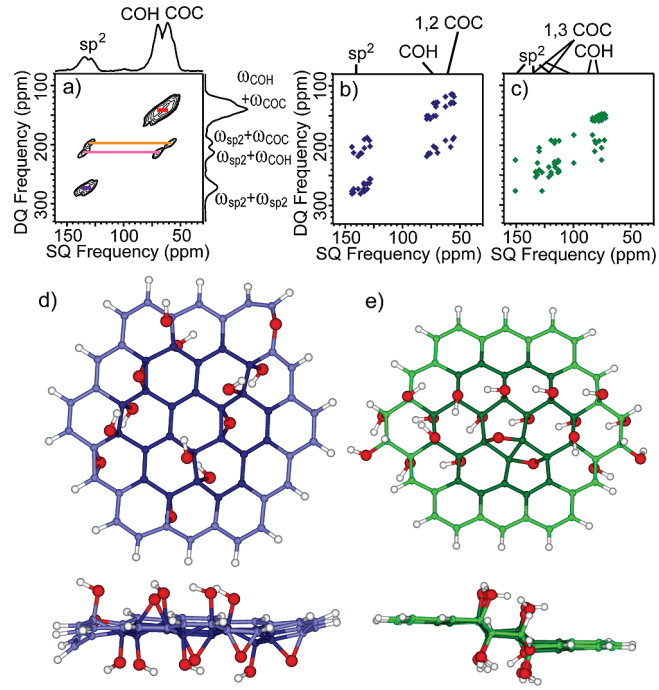

Figure 1. (a) Experimental 2D ^{13}C DQ/SQ correlation SSNMR spectrum of uniformly ^{13}C-labeled GO using ^{13}C−^{13}C *J* coherence transfer. Fast recycling with short recycle delays of 0.3 s and low power (7 kHz) decoupling was used. Signal assignments in (a) are those made in ref 10 and confirmed here. The carrier frequency was set at 211.17 ppm. (b, c) Predicted DQ/SQ correlation spectra based on isotropic chemical shifts calculated for (b) model A and (c) model B. (d, e) Structural models for (d) model A and (e) model B from the (top) top and (bottom) side views. Carbons in (d, e) are color coded to match the spectra in (b, c). Red and white spheres denote O and H, respectively. ^{13}C at the edge of the models (light blue or green) were not included in (b, c). The calculated spectrum (b) based on model A well reproduced the experimental spectrum (a).

Results

Figure 1a shows an experimental two-dimensional (2D) double-quantum/single-quantum (DQ/SQ) ^{13}C-shift correlation spectrum of uniformly ^{13}C-labeled GO (^{13}C > 99%) obtained under magic angle spinning (MAS). In Figure 1a, cross peaks are displayed at $(\omega_{SQ}, \omega_{DQ}) = (\omega_X, \omega_X + \omega_Y)$, where ω_X denotes the ^{13}C SSNMR frequency of the detected carbon $^{13}C_X$ and ω_Y is the frequency of a $^{13}C_Y$ to which a $^{13}C_X$ is correlated via a through-bond *J* coupling (i.e., $^{13}C_X$ and $^{13}C_Y$ are bonded). In our previous work, we demonstrated that sp^2, epoxide (COC), and COH carbons are directly bonded by 2D ^{13}C/^{13}C correlation SSNMR.[10] However, the cross-peaks between ^{13}COH (∼70 ppm) and ^{13}COC carbons (∼60 ppm) were partially obscured by the diagonal peaks. Since diagonal signals are eliminated in the 2D DQ/SQ spectrum, the two cross peaks at $(\omega_{SQ}, \omega_{DQ}) =$ (60, 130 ppm) and (70, 130 ppm) (connected by a red line) confirm unequivocally that the COH and epoxide carbons are directly bonded. Other cross peak pairs show connectivities between epoxide and sp^2 ^{13}C (orange line), ^{13}COH and sp^2 ^{13}C (pink line), and two kinds of sp^2 ^{13}C (purple line). This is consistent with our previous results.

Parts b and c of Figure 1 show simulated 2D DQ/SQ SSNMR spectra based on isotropic ^{13}C chemical shifts obtained by ab initio calculations for (b) model A and (c) model B. Models A and B are cluster models based on the Lerf−Klinowski model[33]

(15) Lipton, A. S.; Heck, R. W.; Ellis, P. D. *J. Am. Chem. Soc.* **2004**, *126*, 4735–4739.
(16) Shaibat, M. A.; Casabianca, L. B.; Wickramasinghe, N. P.; Guggenheim, S.; de Dios, A. C.; Ishii, Y. *J. Am. Chem. Soc.* **2007**, *129*, 10968–10969.
(17) Facelli, J. C.; Nakagawa, B. K.; Orendt, A. M.; Pugmire, R. J. *J. Phys. Chem. A* **2001**, *105*, 7468–7472.
(18) Pooransingh-Margolis, N.; Renirie, R.; Hasan, Z.; Wever, R.; Vega, A. J.; Polenova, T. *J. Am. Chem. Soc.* **2006**, *128*, 5190–5208.
(19) Zhang, Y.; Sun, H. H.; Oldfield, E. *J. Am. Chem. Soc.* **2005**, *127*, 3652–3653.
(20) Kervern, G.; Pintacuda, G.; Zhang, Y.; Oldfield, E.; Roukoss, C.; Kuntz, E.; Herdtweck, E.; Basset, J. M.; Cadars, S.; Lesage, A.; Coperet, C.; Emsley, L. *J. Am. Chem. Soc.* **2006**, *128*, 13545–13552.
(21) Boukhvalov, D. W.; Katsnelson, M. I. *J. Am. Chem. Soc.* **2008**, *130*, 10697–10701.
(22) Cai, D. Y.; Song, M.; Xu, C. X. *Adv. Mater.* **2008**, *20*, 1706–1709.
(23) Cote, L. J.; Kim, F.; Huang, J. X. *J. Am. Chem. Soc.* **2009**, *131*, 1043–1049.
(24) Fan, F. R. F.; Park, S.; Zhu, Y. W.; Ruoff, R. S.; Bard, A. J. *J. Am. Chem. Soc.* **2009**, *131*, 937–939.
(25) Kudin, K. N.; Ozbas, B.; Schniepp, H. C.; Prud'homme, R. K.; Aksay, I. A.; Car, R. *Nano Lett.* **2008**, *8*, 36–41.
(26) Talyzin, A. V.; Solozhenko, V. L.; Kurakevych, O. O.; Szabo, T.; Dekany, I.; Kurnosov, A.; Dmitriev, V. *Angew. Chem., Int. Ed.* **2008**, *47*, 8268–8271.
(27) Stankovich, S.; Dikin, D. A.; Piner, R. D.; Kohlhaas, K. A.; Kleinhammes, A.; Jia, Y.; Wu, Y.; Nguyen, S. T.; Ruoff, R. S. *Carbon* **2007**, *45*, 1558–1565.
(28) Lahaye, R. J. W. E.; Jeong, H. K.; Park, C. Y.; Lee, Y. H. *Phys. Rev. B* **2009**, *79*, 125435.
(29) Park, S.; Lee, K.-S.; Bozoklu, G.; Cai, W.; Nguyen, S. T.; Ruoff, R. S. *ACS Nano* **2008**, *2*, 572–578.
(30) Chen, H.; Muller, M. B.; Gilmore, K. J.; Gallace, G. G.; Li, D. *Adv. Mater.* **2008**, *20*, 3557–3561.
(31) Park, S.; An, J.; Jung, I.; Piner, R. D.; An, S. J.; Li, X.; Velamkanni, A.; Ruoff, R. S. *Nano Lett.* **2009**, *9*, 1593–1597.
(32) Szabo, T.; Berkesi, O.; Forgo, P.; Josepovits, K.; Sanakis, Y.; Petridis, D.; Dekany, I. *Chem. Mater.* **2006**, *18*, 2740–2749.
(33) He, H. Y.; Klinowski, J.; Forster, M.; Lerf, A. *Chem. Phys. Lett.* **1998**, *287*, 53–56.
(34) Mkhoyan, K. A.; Contryman, A. A.; Silcox, J.; Stewart, D. A.; Eda, G.; Mattevi, C.; Miller, S.; Chhowalla, M. *Nano Lett.* **2009**, *9*, 1058–1063.
(35) Schafhaeutl, C. *J. Parkt. Chem* **1840**, *21*, 129.

and Dékány model, respectively.[32] Our previous SSNMR study showed that these two models are the most likely candidates that represent a structure of the GO sample.[10] The geometry-optimized structures of models A and B are shown in parts d and e, respectively, of Figure 1. Model A represents a primarily flat structure (see the side view in Figure 1d, bottom) that is approximately 50% oxidized, with alternating "ribbons" of oxidized and conjugated carbons. Model B is a chairlike structure (see the side view in Figure 1e, bottom) with a band of highly oxidized sites. The latter model lacks 1,2-epoxides and incorporates the 1,3-epoxide motif, as proposed in the Dékány model.[32] In model B, two 1,3-epoxides share a carbon−carbon bond. A similar model having 1,3-epoxide was also proposed by a recent ab initio study.[28] Comparison of Figure 1b,c with Figure 1a shows a much better overall agreement for model A, excluding model B for the present system. In particular, the spectra in Figure 1a,b both show the cross peaks at $\omega_{SQ}\sim$60 ppm, which are absent in Figure 1c for model B. The peaks predicted at $\omega_{SQ}\sim$115 ppm for 1,3-epoxides in Figure 1c are missing in Figure 1a. Figure 1a suggests that sp^2 ^{13}C connected to epoxide (orange line) displays slightly different ^{13}C shifts from those for sp^2 ^{13}C connected to C−OH (pink line); this is reasonably well reproduced in Figure 1b for model A. These findings clearly support model A as the model that best reproduces the experimental spectrum in Figure 1a. We also attempted geometry optimizations beginning with sp^2-conjugated structures containing isolated 1,3-epoxides or 1,4-epoxides, as proposed in the original Dékány model[32] and in a recent transmission electron microscopy study,[34] respectively. However, they were usually optimized to 1,2-epoxides or carbonyl groups. The result is consistent with a recent ab initio study[28] reporting the instability of 1,3-epoxide in graphene in geometry optimization. Since epoxides are often considered to be an unstable species, it is perhaps surprising that our structural modeling approach using SSNMR experiments and ab inito calculations clearly suggested that 1,2-epoxide is likely to be an abundant form in GO.

In previous SSNMR studies of GO, signal assignments were based on solution NMR data for small model compounds.[10,33,36] It is noteworthy that no signal assignment information on GO was utilized in the above analysis to select the best structural model. In fact, in the proposed 2D NMR-based modeling approach using ab initio calculations, prior knowledge on signal assignments is not a prerequisite. A *fingerprint* matching of experimental and simulated 2D spectra allows for the selection of the best-fit structural model, and then calculated shifts for the best model yield assignments with the connectivity information from 2D SSNMR. Thus, this *assignment-free* modeling approach provides a rigorous basis to test signal assignments as well as various structural models for GO and probably other graphite-based systems. This will be particularly useful for the development of new modified graphene/graphite materials, for which signal assignments or NMR shift data for suitable small model compounds may not be easily available.

Multiple quantum (MQ) spectroscopy using *J* coupling such as one in this study has been successfully employed for solids in order to highlight correlations without diagonal signals.[37] However, the requirement of high-power decoupling during the long mixing times generally imposes the use of long recycle delays in order to avoid probe arcing in this method. In our experiments, use of low-power decoupling and the short ^1H T_1 relaxation time of this sample allowed for fast repetition (∼0.3 s/scans) for higher sensitivity (or a better signal-to-noise ratio for a given time).[38] As a result, the 2D spectrum was attained after only 4.5 h for 12 mg of the ^{13}C-labeled sample, rather than 2 days, which would be required by a standard approach with slow recycling. Although systems having slower relaxation times may require more sample quantity, the present approach is likely to be applicable for a broad range of graphite-based systems.

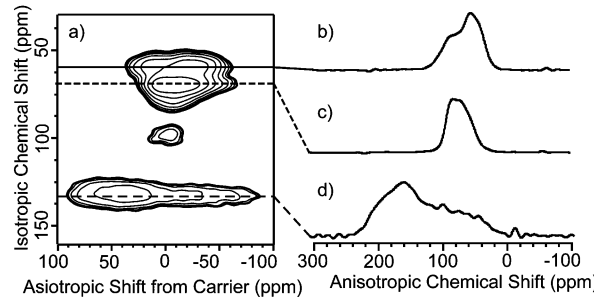

Figure 2. (a) 2D ^{13}C anisotropic chemical shift/isotropic shift correlation spectrum for GO obtained by the ROCSA sequence[42] at 15 kHz MAS with (b−d) 1D slices along the indirect ω_1 dimension showing experimental chemical shift anisotropy (CSA) patterns for (b) COC, (c) COH, and (d) sp^2, found at 60, 70, and 130 ppm, respectively. The horizontal axis of Figure 2a (Anisotropic Shift from Carrier) represents a frequency due to the anisotropic chemical shift under the ROCSA sequence from the carrier frequency, where the carrier frequency (101.9 ppm) is set to 0 ppm. The scale was adjusted by a scaling factor of CSA in the ROCSA sequence (0.272). In the ROCSA sequence, a relatively small contribution of the isotropic shifts still remains in (a). Parts b−d represent CSA patterns after the effect of the isotropic shifts was removed. The assignments are from Figure 1.

In Figure 2, we further confirm the validity of our NMR-based structural model of GO by examining ^{13}C chemical shift anisotropies (CSA). Three principal values of CSA (δ_{11}, δ_{22}, δ_{33}), which can be extracted from these lineshapes, sensitively reflect asymmetry in the local electronic environments.[39−41] Thus, it is possible to test the proposed structural model more rigorously by comparing the principal values calculated at each different carbon site with those from the experimental CSA patterns. Figure 2 shows a 2D spectrum of the ^{13}C-labeled GO correlating isotropic shift and ^{13}C CSA powder patterns, the latter of which was obtained by a ROCSA "recoupling" sequence under MAS.[42] Slices along the indirect dimension show experimental CSA patterns, each of which show singularities (i.e., peaks or shoulders) at principal values. In Figure 3, these slices were compared with powder patterns calculated from the principal values obtained from the ab initio calculations for models A (blue) and B (green) for (a) sp^2, (b) COH, (c) COC. For model B, the powder pattern of 1,3-epoxide ^{13}C does not reproduce the experimental pattern. Although for COH the pattern shows slight deviation probably due to the finite nature of the model, the overall agreement between calculated and

(36) Lerf, A.; He, H. Y.; Forster, M.; Klinowski, J. *J. Phys. Chem. B* **1998**, *102*, 4477–4482.
(37) Fayon, F.; Roiland, C.; Emsley, L.; Massiot, D. *J. Magn. Reson.* **2006**, *179*, 49–57.
(38) Wickramasinghe, N. P.; Parthasarathy, S.; Jones, C. R.; Bhardwaj, C.; Long, F.; Kotecha, M.; Mehboob, S.; Fung, L. W. M.; Past, J.; Samoson, A.; Ishii, Y. *Nat. Meth.* **2009**, *6*, 215–218.
(39) de Dios, A. C.; Oldfield, E. *Solid State Nucl. Magn. Reson.* **1996**, *6*, 101–125.
(40) Walling, A. E.; Pargas, R. E.; de Dios, A. C. *J. Phys. Chem. A* **1997**, *101*, 7299–7303.
(41) Sefzik, T. H.; Turco, D.; Iuliucci, R. J.; Facelli, J. C. *J. Phys. Chem. A* **2005**, *109*, 1180–1187.
(42) Chan, J. C. C.; Tycko, R. *J. Chem. Phys.* **2003**, *118*, 8378–8389.

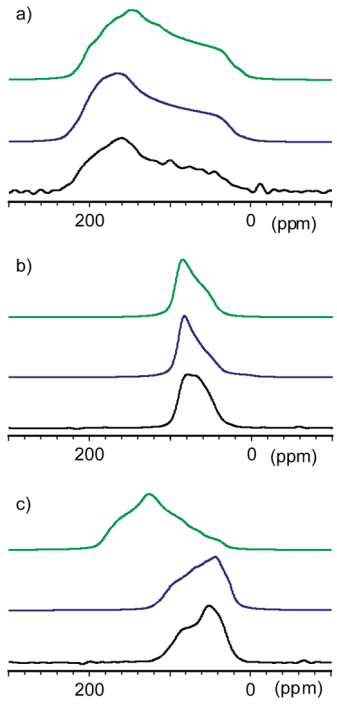

Figure 3. Comparison of the experimental ^{13}C chemical shift anisotropy (CSA) spectrum (black) with simulated CSA powder patterns from ab initio chemical shift calculations (blue, model A; green, model B) for (a) sp^2 and (b) COH (c) COC carbons. The simulated powder patterns were obtained with SPINEVOLUTION software[51] using the principal values predicted by the ab initio calculations performed for Figure 1 as input for the simulations. Contributions of $^{13}C-^{13}C$ dipolar couplings were not included in the simulation. The simulated powder patterns represent a superposition of the carbon sites in each model.

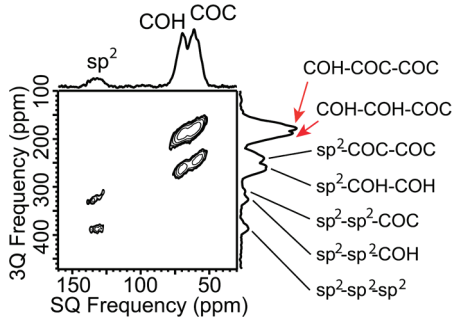

Figure 4. Experimental 2D ^{13}C 3Q/SQ correlation SSNMR spectrum of uniformly ^{13}C-labeled GO using $^{13}C-^{13}C$ *J* coherence transfer. Short recycle delays of 0.3 s and low power (7 kHz) decoupling were used. The carrier frequency was set at 211.17 ppm. In the 3Q frequency dimension, the carrier frequency is displayed as 622.51 ppm so that the 3Q frequency is displayed as the sum of the three SQ frequencies involved in the 3Q coherence. Red arrows denote the presence of 3Q coherence correlating three oxidized ^{13}C sites. See the Methods section for additional details.

experimental spectra is reasonable for model A. Chemical shift calculations including periodic boundaries are ongoing in our laboratory. The results in Figure 3 confirm that model A is likely to present a representative structure of the GO sample analyzed here. On the other hand, for GO oxidized under different conditions, structures such as model B may be present. For such systems, the CSA data for model B can be utilized for future analysis.

Figure 4 shows our preliminary data of a 2D triple-quantum/single-quantum (3Q/SQ) correlation spectrum for the same ^{13}C-labeled GO sample. In this experiment, cross peaks are displayed at $(\omega_{SQ}, \omega_{3Q}) = (\omega_Y, \omega_X + \omega_Y + \omega_Z)$, where ω_Y denotes the ^{13}C SSNMR frequency of the detected carbon $^{13}C_Y$ and ω_X and ω_Z are the frequencies of $^{13}C_X$ and $^{13}C_Z$, to which $^{13}C_Y$ is connected via a through-bond *J* coupling (i.e., connected as $C_X-C_Y-C_Z$). Strong signal intensities were observed for the cross peak correlating three oxidized ^{13}C sites such as 1,2-epoxide and COH (red arrows). The cross peaks clearly demonstrate that a cluster of three oxidized ^{13}C sites is likely to have a considerable population in the GO sample. On the other hand, the presence of 3Q connecting three sp^2 groups seems to indicate that networked sp^2 groups are still retained in this sample. Although further studies are needed, more quantitative analysis of the signal intensities is likely to reveal detailed distributions of the oxidized sites or possible clustering of the oxidized sites in GO and other graphite- and graphene-based systems, including graphene oxide.

Conclusion

We have shown that a combination of multidimensional SSNMR experiments and chemical shift calculations offers a powerful approach to construct a structural model that well reproduces SSNMR spectra for GO. There are primarily three novel aspects in this study. First, the presented approach permits us to fully utilize excellent resolution and connectivity information from multidimensional ^{13}C SSNMR, which has been rarely utilized for graphene/graphite related materials. Without requirements of prior knowledge of NMR chemical shift assignments, this approach will offer a novel means to evaluate structural models of a variety of graphite/graphene-based systems. Based on the results of 3Q/SQ correlation, extending this approach to 3D/4D SSNMR for more detailed structural information is promising with the excellent sensitivity offered by fast recycling under very fast MAS for ^{13}C-labeled GO. Second, the present study on GO is the first example demonstrating that reasonable accuracy in ^{13}C chemical shift calculations can be obtained for infinitely conjugated modified graphene by ab initio calculations for cluster models. As found in the present and previous examples,[14,16,19,20,43] establishing ab initio chemical shift calculations for a new class of materials will open novel opportunities for structural analysis. Chemical shift anisotropy line shapes will offer an additional basis to distinguish different structural models of modified graphene. Third, our results suggest that model A in Figure 1d (based on the Lerf−Klinowski model) convincingly reproduced the 2D DQ/SQ-correlation SSNMR and CSA powder patterns found in our experimental spectra for ^{13}C-labeled GO. Thus, among various models proposed in the previous studies, model A based on the Lerf−Klinowski model is the most plausible structural model for the GO system investigated here. Recently proposed structural models involving 1,3- or 1,4-epoxide moieties, thus, seem not likely to represent the GO system. It is also noteworthy that this study based on the NMR data has revealed the primary structural features for major chemical species in GO, and other kinds of structures may be present at a lower population[44] in the highly heterogeneous sample. Such detailed structural features can be also studied by the present approach if sufficient sensitivity is obtained in NMR data for the minor species. In addition, it is probable that a different degree of oxidization or different oxidization methods may result in GO of different molecular

(43) Le, H.; Pearson, J. G.; Oldfield, E. *J. Am. Chem. Soc.* **1995**, *117*, 3800–3807.
(44) Gao, W.; Alemany, L. B.; Ci, L. J.; Ajayan, P. M. *Nat. Chem.* **2009**, *1*, 403–408.

structures; such structural differences will be easily examined by the method presented here. The characterization of molecular structures of precursors in chemical synthesis often provides a basis to understand the nature of reactions and discover new paths for synthesis. Since the SSNMR approach presented here yields detailed structural information on GO, a precursor for graphene-based systems,[3] and will also be relevant for analysis of other chemically modified graphenes, this approach has value for the synthesis of chemically modified graphene systems and for optimization of such synthesis protocols.

Methods

Solid-State NMR Experiments. Uniformly ^{13}C-labeled graphite oxide was prepared in the Ruoff laboratory as described previously.[10] SSNMR experiments were conducted at 9.4 T using a Varian InfinityPlus 400 NMR spectrometer and a home-built 2.5 mm MAS probe. The pulse sequence and phase cycling used for 2D MQ/SQ correlation experiments through *J* transfer in Figures 1 and 4 are shown in Figure S1 (Supporting Information). All chemical shifts were referenced to TMS using adamantane as an external reference. 2D MQ/SQ correlation spectra in Figures 1a and 4 were collected using a MAS spinning speed of 20000 ± 10 Hz, and the cooling air temperature for a Varian variable-temperature (VT) stack was set at −10 °C. For the spectra of GO shown in Figures 1a and 4, fast recycling with short delays of 0.3 s and low power (7 kHz) decoupling[38] was used. During the CP period, the ^{13}C RF field amplitude was linearly swept from 52 to 70 kHz during a contact time of 2.0 ms, while the ^{1}H RF amplitude was kept constant at 82 kHz.

For the 2D DQ/SQ-correlation experiment in Figure 1a, 200 t_1 points were collected using a mixing time of 1.5 ms with 28 scans for each real or imaginary t_1 data point during a total experimental time of 4.5 h. The t_1 increment was 12.5 μs. The spectra were processed with 150 Hz line Gaussian broadening in each dimension. The carrier frequency for ^{13}C was set at 211.17 ppm. The carrier frequency in the DQ dimension is displayed as 422.34 ppm in Figure 1a so that the DQ frequency simply exhibits the sum of chemical shifts for two correlated ^{13}C groups.

The 2D 3Q/SQ-correlation spectrum on uniformly ^{13}C-labeled GO in Figure 4 was collected with the same pulse sequence used for the 2D DQ/SQ experiment, but with a different phase cycle (see Figure S1, Supporting Information). With a mixing time of 3 ms, 60 t_1 points were collected with 384 scans for each real or imaginary t_1 data point during a total experimental time of 4.5 h. The t_1 increment was 6.25 μs. The carrier frequency for ^{13}C was set at 211.17 ppm. The carrier frequency in the 3Q dimension is displayed as 633.51 ppm in Figure 4 so that the 3Q frequency simply exhibits the sum of chemical shifts for three correlated ^{13}C groups. Other conditions are the same as those for 2D DQ/SQ correlation.

The recoupling of chemical shift anisotropy (ROCSA) pulse sequence developed by Chan and Tycko[42] was used to measure the ^{13}C powder patterns due to chemical shift anisotropy (CSA) of three different chemical groups for GO under magic angle spinning conditions. We used the $C2_2^1$ symmetry sequence with the time period before the first rotor-synchronized pulse (a period as defined in ref 42) and the duration of the composite pulse (b period) equal to $0.0329\tau_R$ and $0.467\tau_R$, respectively, where τ_R denotes a rotation period. The experiment was performed at a spinning speed of 15000 ± 10 Hz. A ^{13}C rf nutation frequency of 64 kHz was used for the ROCSA recoupling period. High-power TPPM ^{1}H decoupling (100 kHz) was used. The cooling air temperature for the VT stack was controlled at −10 °C. For this experiment, 40 t_1 points with 64 scans each were collected using a recycle delay of 2 s, for a total experimental time of 2.85 h.

Ab Initio Geometry Optimization and Chemical Shift Calculations. Chemical shift calculations were performed using Gaussian 03 (Revision D.01)[45] on a Beowulf PC cluster at the Academic Computing and Communications Center at UIC. Each of the models shown in Figure 1 were geometry optimized at the B3LYP/6-31G* level of theory.[46−48] Chemical shielding tensors were calculated using GIAO[49] with B3LYP and a 6-311G basis set. Chemical shieldings for the three principal components of the tensor were converted to chemical shifts as follows. Methane was used as the theoretical reference compound. The isotropic chemical shielding of ^{13}C in methane was calculated at the B3LYP/6-311G level of theory, after geometry optimization at the same level of theory. The calculated shielding was converted to TMS shielding by adding the difference (−11.0 ppm) between the chemical shift of methane in the gas phase and TMS with susceptibility correction.[50] This gave the calculated shielding of TMS, which is 185.0 ppm for B3LYP/6-311G. The calculated shielding tensor values of each carbon were then subtracted from the calculated isotropic shielding of TMS at the same level of theory in order to give the calculated chemical shifts. The principal values of the chemical shift tensors obtained for models A and B are found in the Supporting Information (Table S1). The simulated CSA patterns in Figure 3 were obtained by a superposition of the powder patterns for all ^{13}C sites belonging to the same chemical group.

To create a cluster model from an infinite graphene sheet, we used structures containing 54 carbons terminated with C−H bonds in models A and B. To test whether the conclusion would vary depending on model type, the same calculations were done on alternative models of 43 carbons that were terminated with C−H bonds and C═O groups (models X and Y in Figure S3d,e, Supporting Information). Model X is a model based on the Lerf−Klinowski model, while model Y is that based on the Dékány model. For these slightly smaller models, we simulated 2D DQ/SQ spectra (Figure S3b,c, Supporting Information). A comparison of the experimental spectrum (Figure S3a, Supporting Information) with the simulated spectra supports the conclusion that the model based on the Lerf−Klinowski model (model X in Figure S3d, Supporting Information) best reproduces the experimental spectrum compared to other suggested models.

Acknowledgment. This work was supported by the NSF CAREER program (CHE 449952) and also in part by the Dreyfus Foundation Teacher−Scholar Award program and the NIH RO1 program (AG028490) for Y.I. W.W.C., S.P., R.P., and R.S.R. appreciate support from NSF 0742065, the DARPA CERA and DARPA iMINT Centers, and SWAN-NRI.

Supporting Information Available: Full author list of ref 45, evaluation of ^{13}C chemical shifts for alternative models, and additional details of experimental conditions and ab initio calculations. This material is available free of charge via the Internet at http://pubs.acs.org.

JA9030243

(45) Frisch, M. J. et al. *Gaussian 03 Revision D.01*; Gaussian Inc.: Pittsburgh, PA, 2004.
(46) Becke, A. D. *J. Chem. Phys.* **1993**, *98*, 5648–5652.
(47) Lee, C. T.; Yang, W. T.; Parr, R. G. *Phys. Rev. B* **1988**, *37*, 785–789.
(48) Hariharan, P. C.; Pople, J. A. *Theor. Chim. Acta* **1973**, *28*, 213–222.
(49) Ditchfield, R. *Mol. Phys.* **1974**, *27*, 789–807.
(50) Jameson, A. K.; Jameson, C. J. *Chem. Phys. Lett.* **1987**, *134*, 461–466.
(51) Veshtort, M.; Griffin, R. G. *J. Magn. Reson.* **2006**, *178*, 248–282.